Energy materials

Research on the structure-performance relationship of thermal reduced graphene oxide based supercapacitors

Peng Zhang[1], Kunjie Wang[1], Xianrong Liu[1], Li Wang[2], and Wensheng Gao[3,*]

[1] *Qinghai Provincial Key Laboratory of New Light Alloys, Qinghai Provincial Engineering Research Center of High-Performance Light Metal Alloys and Forming, Qinghai University, Xining 810016, People's Republic of China*
[2] *College of Chemistry and Chemical Engineering, Xi' an Shiyou University, Xi'an 710065, People's Republic of China*
[3] *Advanced Catalysis Center, College of Chemistry and Chemical Engineering, Lanzhou University, Lanzhou 730000, China*

ABSTRACT

The electrochemical performance of RGO-based super-capacitors are highly dependent on the exfoliation and surface functionalization degree of RGO, which of them contributes to the capacitance and pseudo-capacitance of the electrode materials respectively. In this work, a series of tRGO samples were fabricated as the raw material of graphite oxide (GO) by thermal expansion method through precisely controlling its thermal expansion temperature. It is founded that the specific capacitance of tRGO gradually decreased with the increasing of the thermal treatment temperature. Especially, the tRGO fabricated by the lowest heat treatment temperature (150 °C) exhibited the largest specific capacitance (326 Fg^{-1}) for three-electrode with the loading of 1.5 mg in 6 M KOH electrolyte. Based on the optimized result of tRGO-150, which exhibited the specific capacitance of 202 Fg^{-1} for the two-electrode symmetrical capacitor with the loading of 7.3 mg. The heat treatment temperature has the greatest influence on the C=O% than electrical conductivity and pore structure, thereby determine the specific capacitance for tRGO based super-capacitors.

Introduction

With the increasingly worsening situations of fossil fuel depletion and global warming, developing the renewable energy sources and upgrading energy storage strategies continue to be the top priority for mankind in future [1]. Among them, the energy storage is necessary to the effective utilization of the produced renewable energies [2–4]. Super-capacitors, has gradually become one of the most important energy storage devices used in new-energy vehicles,

---

Handling Editor: Joshua Tong.

Address correspondence to E-mail: gaowsh13@lzu.edu.cn

🌱 Springer

and continues to attract a large amount of research attentions relying on their high power densities, rapid charging/discharging characteristic and excellent cycle life [5–7]. Especially in recent years, in addition to further improving the energy density, cost-effective large scale production has become more of the relevant research consideration driven by actual needs.

Graphene based materials have been extensively investigated as the electrode material for supercapacitors because of their high specific surface areas and high electric conductivity and theoretical specific capacitance (550 Fg^{-1}) [8–10]. Nevertheless, the sheet restacking and aggregation issues limit the success of the application of graphene in supercapacitors. In recent years, much researches has been devoted to the development of exfoliated three-dimensional (3D) porous graphene nanostructure used in supercapacitors [11, 12]. These exfoliated porous graphene nanostructures are generally prepared through hydrothermal processes, self-assembling, sol−gel processes, thermally expansion routes and so on [13, 14]. These strategies have successfully produced 3D porous graphene nanostructures of high specific surface areas, high porosities and rich functional groups. Among them, the thermal exfoliation method displays the obvious advantage by taking care of time-consuming, energy-consuming, process complexity and scalability. As reported by McAllister et al., they suggest a critical temperature of 550 °C for exfoliation of GO to occur, and the full exfoliation for RGO is normally need above 1000 °C, which result the huge specific surface area (SSA), large porous structure, high reduction degree and the poor oxygen-containing groups [15]. Those characteristics endow the RGO with high good double layer capacitive (DLC) behavior but poor pseudocapacitive (PC) behavior. In order to balance the surface chemistry and porous structure for RGO, Yang et al., reported a low-temperature thermally reduced strategy at 200 °C with the assist of high vacuum, the obtained RGO owning rich oxygen-containing group couple with huge porous structure shows high capacitance and excellent power capability [16]. In addition, they conclude that different surface chemistry leads to entirely different electrochemical behaviors. The above works suggest that designed RGO with rich surface functional groups coupled with huge porous structure is an effective strategy to maximize its electrochemical properties by balancing

the DLC behavior and pseudocapacitive in aqueous super-capacitor applications. Specially, the influence factor of the RGO intrinsic properties on the electrochemical performance is main including the electrical conductivity, porous structure and pseudo capacitance-contributed group content [17–19]. Despite recent studies, little research of the relationship between the thermal treatment temperature and the electrochemical performance of RGO. In our recent exploration for thermal-exfoliation RGO, we developed a low temperature thermal reduction method without the assist of the high vacuum to obtain a serious of RGO with the designed size and surface modification, [20, 21] which demonstrated the obvious size effect and interface effect in energy storage [22] and polymer nano-composites [23]. However, the effect of the thermal treatment temperature on the intrinsic properties and electrochemical performance of the RGO is still lacking. What's more, investigating the main influence factor on electrochemical performance of RGO has an important guiding significance for scale production and application in super-capacitor field.

In this work, the thermal-exfoliation RGO (tRGO) through gradient heat treatment temperature was fabricated by using GO as the precursor, as shown in Scheme 1. The influence of the thermal exfoliation temperature on the electrical conductivity, porous structure and surface chemistry of tRGO were systemically studied by the corresponding characterization methods. Furthermore, the effect of the intrinsic influence factor of tRGO on the electrochemical performance in super-capacitor was given by optimizing the electrochemical performance test results. This work highlights the need to adapt the heat treatment temperature of tRGO to realize a balance between porous structure and functionalization for optimizing the capacitance and the energy density.

Experimental section

Preparation of GO

The precursor GO was prepared with modified Hummers method. Briefly, 5 g graphite flakes (99 mesh in this work) were put into concentrated H_2SO_4 (200 mL) and kept in an ice bath (< 5 °C). $KMnO_4$ (150 g) was slowly added under stirring in order to
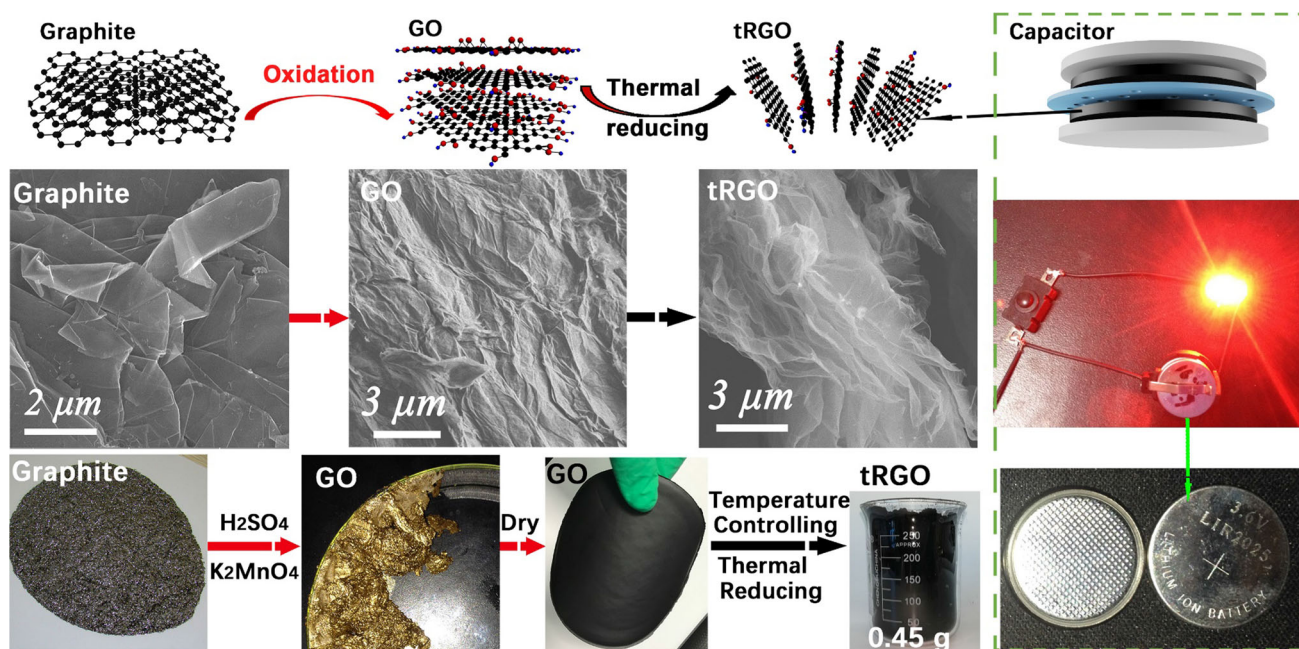
Scheme 1 Schematic illustrating a procedure to fabricate tRGO based supercapacitors.

keep the temperature of the mixture below 30 °C. After stirring for 24 h, the mixture was slowly diluted in 3 L distilled water. Then 30% H_2O_2 solution (50 mL) was added to the mixture slowly until the mixture turned bright yellow while bubbling. The mixture coagulated and washed several times with 5–10% HCl solution for removing the remained metal and sulfate ions. Eventually, the graphite oxide was dried at 35 °C for 72 h.

Preparation of tRGO

The tRGO was synthesized by an optimized thermal reduced methods [20] as the raw material of above GO under an argon protection. The whole process involves three steps. Firstly, GO was kept for 5–10 min at a designed preset temperature 80 °C. Then GO was rapidly heated to the designed temperature in the shortest possible time (**Caution**: slight explosion phenomenon occurred some seconds later). Lastly, the expanded product was collected and further dried at 80 °C to remove the residual water and HCl. The samples was named as tRGO-150, tRGO-200, tRGO-400 corresponding to the designed thermal treatment temperature of 150 °C, 200 °C, 400 °C respectively. The other samples with higher thermal treatment temperature was directly produced from GO via ultra-rapid thermal treatment at the designed temperature under an argon protection. They were

named as tRGO-600, tRGO-800 and tRGO-1000 corresponding to the thermal treatment temperature of 600, 800 and 1000 °C, respectively.

Sample characterization

Chemical composition analysis of the tRGO samples were carried out using X-ray photoelectron spectroscopy (XPS, ESCALAB 250). The nature of the bonding was characterized with a Nicolet NEXUS 670 Fourier transform infrared spectroscope and Raman spectroscopic (Horiba Jobin Yvon LABRAM-HR800 with a wavelength range of 0–4000 cm^{-1}). The morphology of the samples were investigated by a Scanning Electron Microscopy (SEM-S4800). The surface area and pore structure of the samples were measured by N_2 adsorption at 77 K using the BET method on a MICROMERITICS TriStarII 3020 surface analyzer.

Electrochemical Measurements

The electrochemical performance was tested by cyclic voltammetry (CV), galvanostatic charge–discharge (GCD) and electrochemical impedance spectroscopy (EIS) on a CHI 660 E electrochemical workstation (Chenhua, Shanghai, China). The electrode materials consist of 80 wt.% tRGO, 10 wt.% Ketjenblack (EC-300 J) and 10 wt.% PTFE. Electrochemical properties

of designed tRGO were measured with an aqueous system in 6 M KOH with a mass loading of 1.6 mg, and two-electrode symmetric super-capacitors (as shown in Scheme 1) were assembled to evaluate the super-capacitive performance of the tRGO-150 with the mass loading on each electrode of 7.3 mg.

Results and discussions

Characterization of samples

Scheme 1 demonstrates the synthesis process of the tRGO, the layer structure was fully exfoliated after oxidation and thermal expansion. It occurs the great transformation in the appearance color and microstructure due to the change of the chemical composition and condensed structure as shown in Scheme 1. SEM images (Fig. 1) revealed the morphology of designed tRGO, which exhibited the typical exfoliated laminated structure. It's worth noting that the tRGO fabricated under higher temperature displayed the relatively more open hierarchical structure as shown in Fig. 1d, e, f and Fig. 1a, b, c. This subtle difference is further supported by the results of the BET specific surface area (SSA) characterization. The designed tRGO samples with gradient pore structures were evaluated by N_2 adsorption and the corresponding adsorption–desorption isotherms as shown in Fig. 2a. Clearly, the samples exhibited a typical type-IV adsorption

isotherms [24]. As shown in Fig. 2b, the BET SSA were calculated as 235.1, 237.6, 256.2, 267.7, 279.1 and 276.9 m^2g^{-1} for tRGO-150, tRGO-150, tRGO-200, tRGO-400, tRGO-600, tRGO-800 and tRGO-1000, respectively. The total volume adsorbed increased with the heat treatment temperature, reflecting the development of pore structure as a result of Fig. 1. The high temperature treated tRGO owns the higher SSA values, the SSA values gradually increased with the improving of the thermal treatment temperature. In particular, there is liner correlation between SSA and thermal treatment temperature of the tRGO as following:

$$SSA = 225.2 + 0.069T$$

where T is the degree Fahrenheit, which is less than 800 °C. This changing trend is inconsistent with previous observations, the higher thermal expansion rate results the more opened porous structure by thermal reduction methods. An existing thermal expansion mechanism [25] and our previous work [21] indicates exfoliation degree of tRGO is mainly determined by the decomposition rate of oxygen-containing groups and the yielding pressures. In this experiment, the higher treatment temperature reduces the more rapid gas evolution due to the thermal deposition of oxygen-containing groups on GO, in which the higher interlayer pressure contribute to the higher SSA and exfoliation degree.

The exfoliation degree of the obtained tRGO samples were further characterized by X-ray diffraction

Figure 1 The SEM images of temperature-dependent tRGO. **a** tRGO-150; **b** tRGO-200; **c** tRGO-400; **d** tRGO-600; **e** tRGO-800; **f** tRGO-1000.
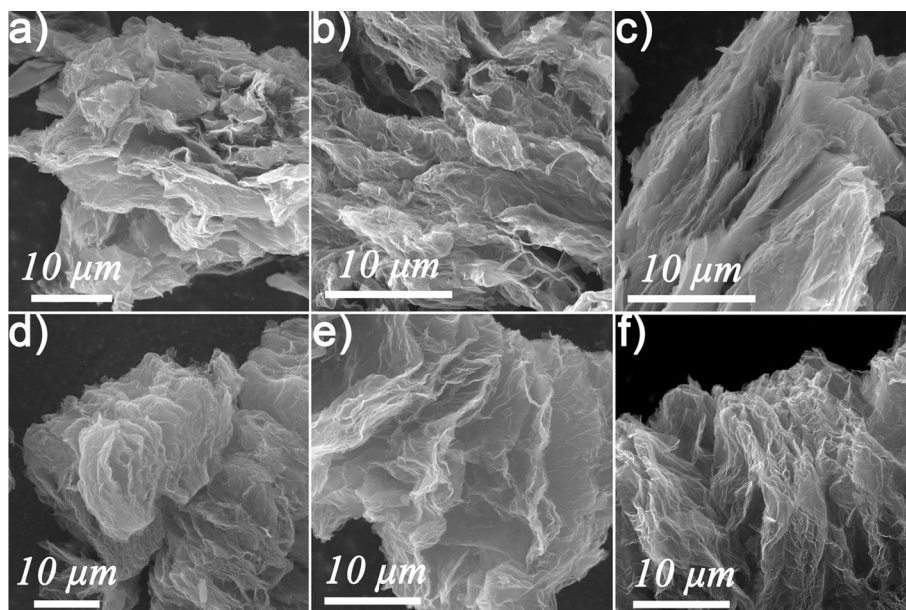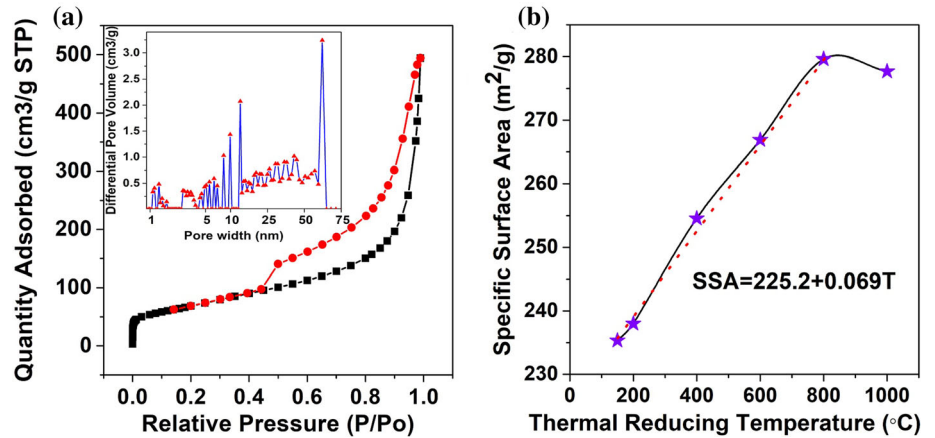
Figure 2 The adsorption–desorption curve attaching DFT pore size distribution **a** and SSA valuues with respect to heat treatment temperature **b** of the designed tRGO.

(XRD). As shown in Fig. 3a, through the Hummers method oxidation, the GO shows a typical (002) peak located at 12.4° in XRD pattern, corresponding to an interlayer spacing of 0.77 nm. After the low temperature thermal expansion, the sharp peak around 12.4° disappears and a broad peak gradually shifts 26.5°, which indicates that oxygen stacked interlayer is largely removed and the tRGO trends to graphitization with the increasing of the heat treatment temperature. Simultaneously, the chemical composition also obviously changed as demonstrated through FT-IR spectra in Fig. 3b, the peaks corresponding to the $^{\nu}$(C=O) and $^{\nu}$(OH) gradually become weaker with the increasing the heat treatment temperature due the decomposition of oxygen-containing groups on GO under high temperature.

The Raman spectra of tRGO are similar with the GO, with the presence of a high and board D band [26] as shown in Fig. 4a. The board Raman peak (D band) indicates a characteristic feature of defects induced in the graphitic structure and functional groups attached on the surface of tRGO. Especially, after fitting the D and G band, the I_D/I_G Raman peak ratios (disorder) gradually decreased with the increasing of the heat treatment temperature, which is due to the restructure of the graphene at high temperature. To further quantitatively investigate the changing of chemical property of tRGO, the chemical group ratio was measured by XPS spectra. As shown in the Gaussian fitting spectrum of tRGO in Fig. 4b, the ratio of C=O group gradually decreased with the increasing of the heat treatment temperature due to the same reason of FT-IR result. According to the C 1 s fitting spectrum and FT-IR spectra, the tRGO-150 fabricated under low heat treatment temperature owns more C=O group, which is believed to contribute more pseudo capacitance.

Figure 3 The XRD patterns **a** and FT-IR spectrums **b** of the designed tRGO.
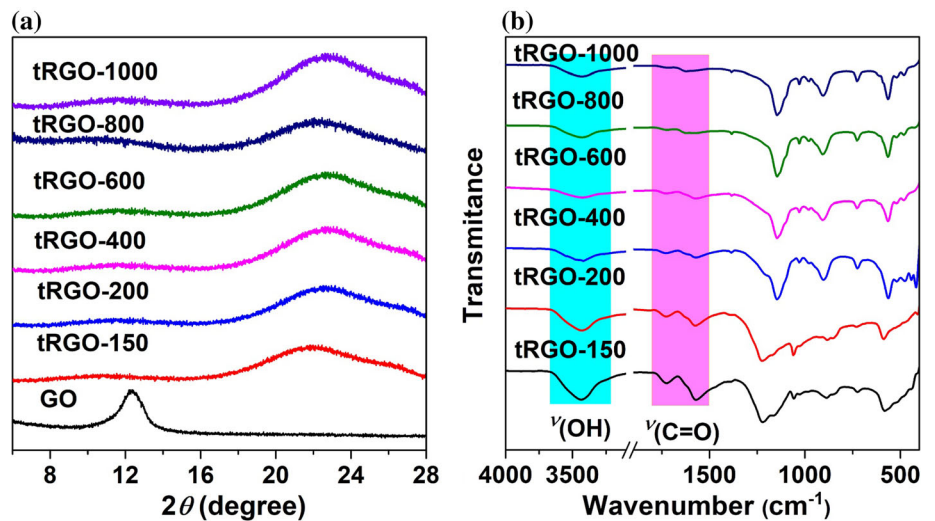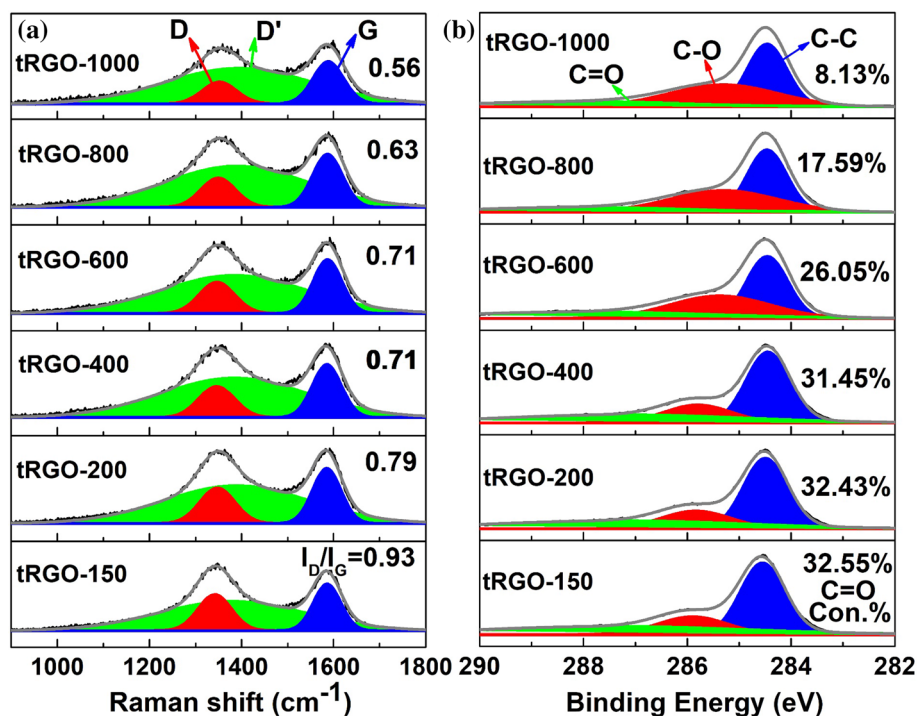
Figure 4 The Raman sepctrums **a** and XPS C1s fitting spectrums **b** of the designed tRGO.

Electrochemical performance

The capacitive behavior of tRGO samples was firstly explored in a three-electrode system using 6 M KOH as electrolyte. As shown in Fig. 5a, CV curves of all tRGO samples at the scan rate of 100 mVs^{-1} exhibit the typical quasi-rectangular shapes with heavy distortions. As a typical sample, the tRGO-150 exhibited an obvious synergic effect of the DLC behavior and pseudocapacitive behavior contributed from oxygen-containing redox region as shown in Fig. 5f. Especially, tRGO-150 displays the largest specific capacitance relying on the exfoliated hierarchical structure and high ratio of C=O group, the latter could provide more charge storage sites and fast ion transport characteristics due to the high electrolytic characteristic. Notably, with the improvement of the heat treatment temperature, the CV curves of tRGO gradually trends to the relative standard rectangular shapes because of the excellent conductivity (Fig. 5e) and decreasing oxygen-containing groups. To further explore the effect of the heat treatment temperature on the electrochemical behaviors, galvanostatic charge/discharge (GCD) test were employed for all tRGO at the current density of 1Ag^{-1} (Fig. 5b). The electrochemical stability of the tRGO was tested by GCD test for 10,000 cycles at 5 Ag^{-1} as shown in Fig. 5c. The specific capacitance of tRGO-150 reaches 326 Fg^{-1}, with the improving of the heat treatment temperature, the specific capacitance gradually decreased (Fig. 5d). The tRGO-150 showed 81.2% capacitance retention over 10,000 cycles (Fig. 5d), indicates the optimized electrochemical stability. The reason for the gradually decreased capacitance mainly due to the lower redox reactions for tRGO at higher heat treatment temperature, which deliver lower pseudo capacitance even although they own higher SSA value and electric conductivity (Fig. 5e). As concluded, the high thermal expansion temperature resulted in high surface area and high electrical conductivity of RGO, which will also lead to lower surface functional groups of RGO simultaneously, the surface functional groups can provide additional pseudo capacitance.

Based on the best result of the electrochemical performance of designed tRGO, the tRGO-150 was employed to assemble the capacitors as the electrode material, which is explored in a two-electrode system using 6 M KOH as electrolyte. The capacitive performances of the tRGO//tRGO symmetrical capacitor was evaluated by CV scans, GCD tests and electrochemical impedance. Figure 6a shows the high rate capability of tRGO//tRGO symmetrical capacitor with the scan rate increasing from 5 to 100 mVs^{-1}. The tRGO//tRGO symmetrical capacitor exhibits excellent high rate capability by maintaining the
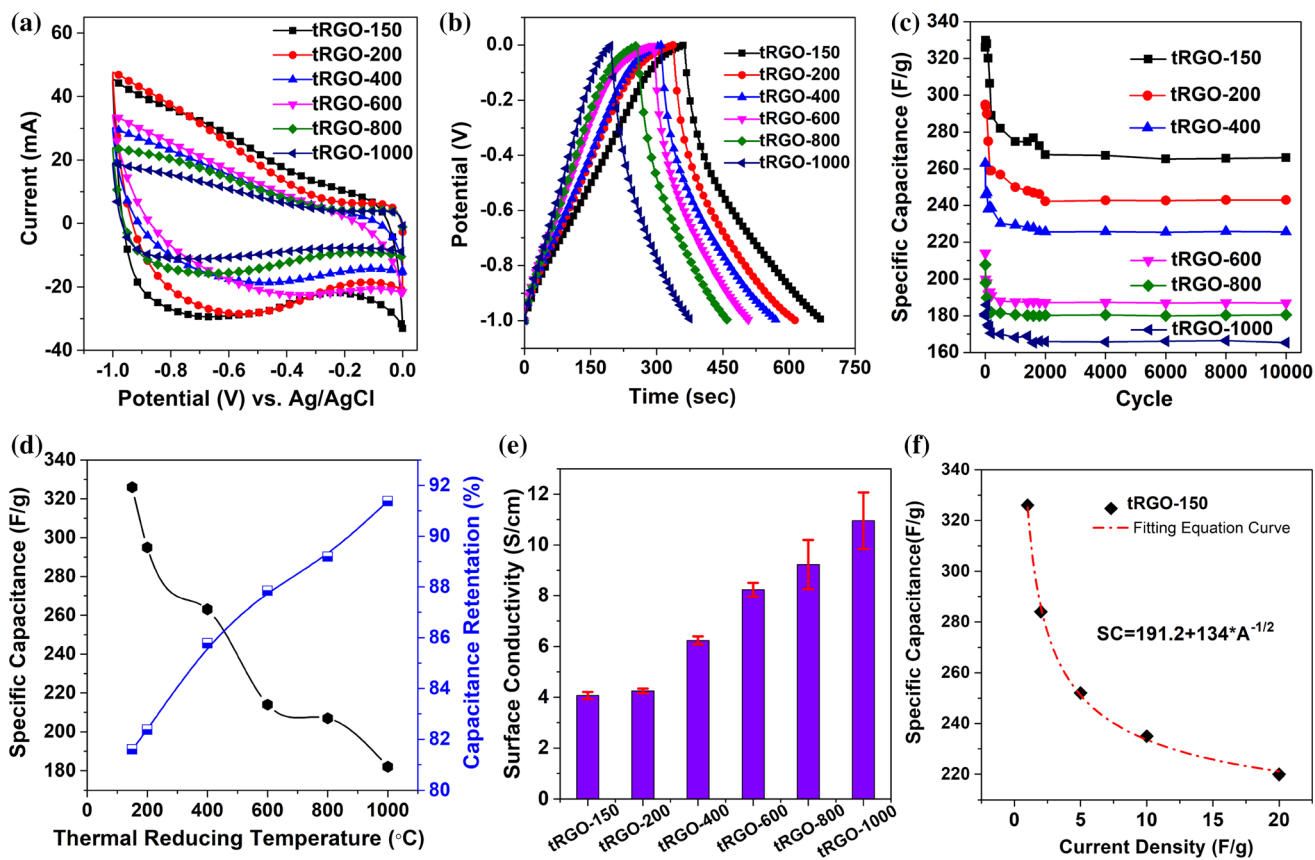
Figure 5 Electrochemical performance of designed tRGO in 6.0 M KOH electrolyte. **a** CV curves of all tRGO at the scan rate of 100 mVs^{-1}; **b** GCD curves of all tRGO at the current densities of 1.0 Ag^{-1}; **c** Cyclic stability of the tRGO in 6.0 M KOH after ten thousand cycles at 5 Ag^{-1} with a voltage window of 1 V; **d** the specific capacitance and capacitance retention of the tRGO respects to the changing of the thermal treatment temperature; **e** the conductivity versus thermal treatment temperature of tRGO; **f** the specific capacitance of the tRGO-150 versus current.

symmetric rectangular shape of the CV loops even at the high scan rate of 100 mVs^{-1}, demonstrating excellent rate capability and fast charge-propagation capability. In addition, the tRGO//tRGO symmetrical capacitor exhibits the excellent rate capability demonstrated from the GCD curves as shown in Fig. 6b, the specific capacitance of tRGO//tRGO reaches 202 Fg^{-1}, 180 Fg^{-1} and 150 Fg^{-1} at 1 Ag^{-1}, 2 Ag^{-1} and 5 Ag^{-1}, respectively. Besides, the electrochemical stability of the tRGO//tRGO was tested by GCD test for 10,000 cycles at 5 Ag^{-1} as shown in Fig. 6c. After 10,000 cycles, the tRGO//tRGO showed 81.2% capacitance retention due to the excellent stability of the RGO. To further understand the superior performance of tRGO//tRGO symmetrical capacitor, electrochemical impedance spectroscopy (EIS) test was also used to reveal the electrolyte ion transport properties. As shown in Fig. 6d (Nyquist plot), the low frequency region presents nearly straight line,

indicating good double layer capacitive behavior couple with pseudocapacitive behavior. Usually the high frequency region is related to the charge/ion transfer resistance between the electrode materials and electrolytes [26], which is influenced by the material porosity and thickness. Similar to the three-electrode system (Fig. 5f), the tRGO-150 based two electrode symmetrical capacitor also exhibited an obvious synergic effect of the DLC behavior and pseudocapacitive behavior contributed from oxygen-containing redox region as shown in Fig. 6e. It is noted that the capacitance of the tRGO is higher than most of those observed for thermal reduced GO [27–33]. The above results suggest that the synergistic effect of the conductivity and oxygen-containing functional groups is vital to performing high specific capacitance for pure carbon electrode materials.
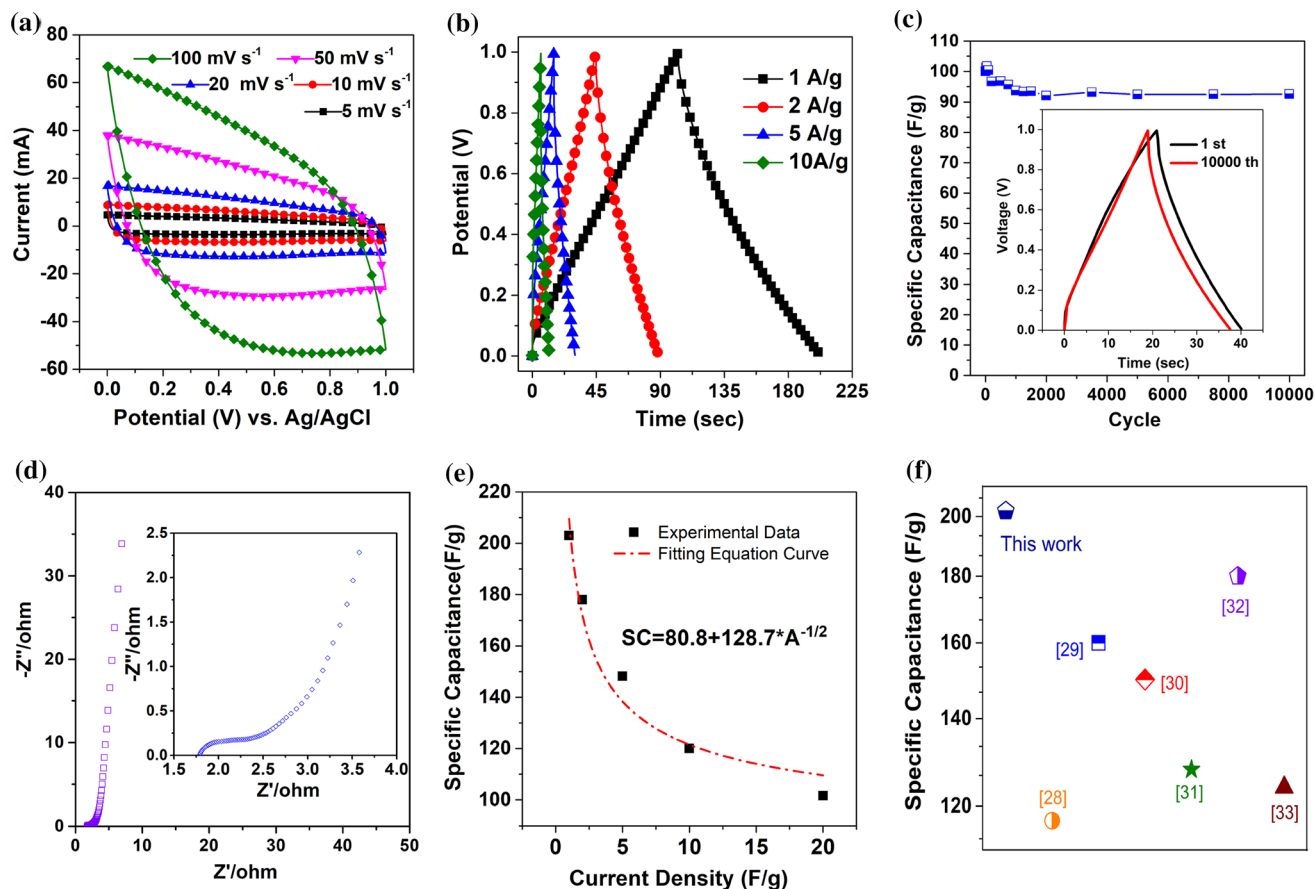
Figure 6 Electrochemical performance of tRGO-150 symmetrical cell in 6.0 M KOH electrolyte. **a** CV curves of the cell operated at different scan rate at the voltage ranges of 1 V; **b** GCD curves of the cell at various current densities; **c** Cyclic stability of the cell in 6.0 M KOH after ten thousand cycles at 5 Ag^{-1} with a voltage window of 1 V; **d** Nyquist plots of the symmetrical cell. Inset magnifies the high-frequency range; **e** the specific capacitance of the tRGO-150 versus current; **f** Comparison of the specific capacitance for tRGO-150 with other thermal reduced RGO reduced at 1 Ag^{-1} in two electrode symmetrical cell.

Conclusion

In summary, a promising energy storage material with high energy density for high performance super-capacitor was provided by using environmentally low-temperature thermal reduction method. The effect of heat treatment temperature on the electrochemical performance of designed tRGO was comprehensively demonstrated. By utilization of the high charge storage sites and fast ion transport characteristics, the tRGO fabricated by lowest heat treatment temperature (150 °C) exhibit the highest specific capacitance and energy density as electrode material. The specific capacitances of 202−150 Fg^{-1} at current densities of 1−5 Ag^{-1} in the potential window of 0−1 V are obtained in a two-electrode system using 6 M KOH as electrolyte with 7.3 mg electrode materials loading. The high cycling stability of 81.2% is also achieved after 10,000 cycles at a current density of 5 Ag^{-1}. This work shows a clear strategy for finely controlling the conductivity and density of functionalities on tRGO for applications in energy storage and conversion fields via a green and energy-efficient process.

Declarations

Conflict of interest All the authors that they have no conflict of interest.

References

[1] Wang CC, Liang J, Liao YH, Lu SY, Sustain ACS (2017) Chem Eng 5:4457

[2] Wang F, Wu X, Yuan X, Liu Z, Zhang Y, Fu L, Zhu Y, Zhou Q, Wu Y, Huang W (2017) Chem Soc Rev 46:6816

[3] Zhang Y, He J, Gao Z, Li X (2019) Nano Energy 65:104045

[4] Liu L, Niu Z, Chen J (2016) Chem Soc Rev 45:4340

[5] Yan J, Wang Q, Wei T, Fan Z (2014) Adv Energy Mater 4:1300816

[6] Muzaffar A, Ahamed MB, Deshmukh K, Thirumalai J (2019) Renew Sust Energ Rev 101:123

[7] Liu S, Wei L, Wang H (2020) Appl Energ 278:115436

[8] Kaempgen M, Chan CK, Ma J, Cui Y, Gruner G (1872) Nano Lett 2009:9

[9] Rani JR, Thangavel R, Oh SI, Woo JM, Das NC, Kim SY, Lee YS, Jang JH, Appl ACS (2017) Mater Interfaces 9:22398

[10] Xiong P, Zhu J, Zhang L, Wang X (2016) Nanoscale Horiz 1:340

[11] Strauss V, Marsh K, Kowal MD, Kady MEl, Kaner RB (2018) Adv Mater 30:1704449

[12] Meng Y, Wang K, Zhang Y, Wei Z (2013) Adv Mater 25:6985

[13] Huang Y, Liang J, Chen Y (1805) Small 2012:8

[14] Guirguis A, Maina JW, Zhang X, Henderson LC, Kong L, Shon H, Dumée LF (2020) Mater Horizons 7:1218

[15] Xie Y, McAllister SD, Hyde SA, Sundararajan JP, Fouetio Kengne BA, McIlroy DN, Cheng IF (2012) J Mater Chem 22:5723

[16] Zhang C, Lv W, Xie X, Tang D, Liu C, Yang QH (2013) Carbon 62:11

[17] Lyu J, Mayyas M, Salim O, Zhu H, Chu D, Joshi RK (2019) Mater Today Energy 13:277

[18] Zhang H, Yang D, Lau A, Ma T, Lin H, Jia B (2021) Small 17:2007311

[19] Yang Z, Tian J, Yin Z, Cui C, Qian W, Wei F (2019) Carbon 141:467

[20] Gao W, Li J, Yan X, Zhu B, Jia J, Huang A, Bai Y (2017) RSC Adv 7:31085

[21] Gao W, Lu Y, Chao Y, Ma Y, Zhu B, Jia J, Bai Y (2017) J Phys Chem C 121:21685

[22] Chen S, Gao W, Chao Y, Ma Y, Zhang Y, Ren N, Bai Y (2018) Electrochim Acta 273:181

[23] Gao W, Ma Y, Zhang Y, Chen Q, Chen H, Zhu B, Bai Y (2018) Compos Part A Appl Sci Manuf 107:479

[24] Yang SJ, Kim T, Jung H, Chong RP (2013) Carbon 53:73

[25] Ganganboina AB, Dutta Chowdhury A, Doong RA (2017) ACS Sustain Chem Eng 5:4930

[26] Donohue MD, Aranovich GL (1998) Adv Coll Interface Sci 76:137

[27] Down MP, Rowley-Neale SJ, Smith GC, Banks CE, Appl ACS (2018) Energy Mater 1:707

[28] Vivekchand SRC, Rout CS, Subrahmanyam KS, Govindaraj A, Rao CNR (2008) J Chem Sci 120:9

[29] Azhari A, Marzbanrad E, Yilman D, Toyserkani E, Pope MA (2017) Carbon 119:257

[30] Luo J, Jang HD, Huang J (2013) ACS Nano 7:1464

[31] Ye J, Zhang H, Chen Y, Cheng Z, Hu L, Ran Q (2012) Power Sources 212:105–110

[32] Bai Y, Rakhi RBB, Chen W, Alshareef HNN (2013) J Power Sources 233:313–319

[33] Chen S, Ma W, Cheng Y, Weng Z, Sun B, Wang L, Chen W, Li F, Zhu M, Cheng HM (2015) Nano Energy 15:642